International Journal of Pharmaceutics 386 (2010) 61–70

Contents lists available at ScienceDirect

International Journal of Pharmaceutics

journal homepage: www.elsevier.com/locate/ijpharm

Understanding polymer–lipid solid dispersions—The properties of incorporated lipids govern the crystallisation behaviour of PEG

Johan Unga[a,*], Pär Matsson[b], Denny Mahlin[b]

[a] Department of Chemical and Biological Engineering, Chalmers University of Technology, Göteborg, Sweden
[b] Department of Pharmacy, Uppsala University, Uppsala, Sweden

ARTICLE INFO

Article history:
Received 8 July 2009
Received in revised form 24 October 2009
Accepted 29 October 2009
Available online 10 November 2009

Keywords:
Lipids
Polyethylene glycol
Solid state
Solid dispersions
Stability
Multivariate data analysis
Principal component analysis
Partial least squares projection to latent structures

ABSTRACT

A deeper insight into the crystallisation process of semi-crystalline polymers during formation of solid dispersions is crucial to improve control of product qualities in drug formulation. In this study we used PEG 4000 with 12 different lipids as a model system to study the effect that incorporated components may have on the crystallisation of the polymer. The lipids were melted with PEG 4000 and the crystallisation of the polymer studied with differential scanning calorimetry (DSC) and small angle X-ray diffraction (SAXD). PEG 4000 can crystallise into lamellar structures with either folded or fully extended polymer chains. All lipids increased the fraction of the folded form and lowered the crystallisation temperatures. Some lipids were incorporated to a high extent into the amorphous domains of the PEG lamellae and thereby swelling the structure, which also resulted in a high degree of chain folding. Partial least squares (PLS) modelling indicated that small hydrophilic lipids increased the folding of PEG and that large non-polar lipids retarded the unfolding during secondary crystallisation. This work shows that there is a large difference in the behaviour of PEG depending on lipid added. Differences are explained in terms of molecular properties for the lipids, demonstrated by the use of PLS modelling to describe the behaviour of PEG solid dispersions.

1. Introduction

The solubility problem of many new drug candidates remains a challenge within pharmaceutical development (Stegemann et al., 2007). The concept of solid dispersions is one formulation strategy utilized to improve bioavailability of poorly soluble compounds. The properties and performance of solid dispersions of poorly soluble drugs has therefore been explored now for some decades (Chiou and Riegelmann, 1971; Leuner and Dressman, 2000; Serajuddin, 1999). A solid dispersion normally consists of two components; the carrier and a dispersed active compound. The dissolution of the active compound is to a high degree dependent on the degree of its dispersion in the solid carrier. Hence, attempts have been made to increase the degree of drug dispersion by adding surfactants to the carrier (Alden et al., 1992; Morris et al., 1992).

The recent introduction of the hot melt extrusion technique as a tool for producing pharmaceutical formulations has further boosted the interest for solid dispersions. Hot melt extrusion enables incorporation of hydrophobic substances in polymeric and/or lipid carriers without the use of solvents and has a great potential for industrial production (Crowley et al., 2007; Leuner and Dressman, 2000; Nakamichi et al., 2002). Recently, Li et al. (2009) have utilized this technique to produce a 'preconcentrate' which is similar to the concept of 'dry emulsions' (Pedersen et al., 1998; Takeuchi et al., 1992). In such formulations the drug is dissolved in a lipid which in turn is dispersed in a soluble carrier matrix with the aid of surfactants.

For a solid dispersion to be suitable as a pharmaceutical product it needs to show improved dissolution of an incorporated drug and, still, be stable on storage. Commonly the dissolution profile of the drug in a solid dispersion changes on storage due to physical instability which imposes phase separations and re-crystallisations of the dispersed components (Dordunoo et al., 1997; Smikalla and Urbanetz, 2007; Urbanetz, 2006) but examples where storage do not influence the release profile have also been reported (Verheyen et al., 2004). To achieve predictive and rational strategies for formulation of solid dispersion it is imperative to have a fundamental understanding of the structure and dynamics of the multi phase system which is formed when a hydrophobic component is mixed with the hydrophilic carrier.

Polymers used as carrier in solid dispersions prepared by hot melt extrusion, should have a relatively low melting point. Polyethylene glycol (PEG) is such a polymer that has been used numerous times both in actual products and as carrier model in

* Corresponding author. Present address: Department of Physical and Analytical Chemistry, BMC Box 579, Uppsala University, SE-751 23 Uppsala, Sweden.
Tel.: +46 18 471 3655; fax: +46 18 471 3654.
E-mail address: johan.unga@fki.uu.se (J. Unga).

0378-5173/$ – see front matter © 2009 Elsevier B.V. All rights reserved.
doi:10.1016/j.ijpharm.2009.10.049

more fundamental research (Dordunoo et al., 1997; Smikalla and Urbanetz, 2007; Saers et al., 1993; Serajuddin, 1999; Bartsch and Griesser, 2004; Leuner and Dressman, 2000). The solid state of pure polyethylene glycol (PEG) has been extensively studied (Spegt, 1970; Buckley and Kovacs, 1975, 1976). PEG forms lamellar semi-crystalline structures where each polymer molecule can be folded a number of times. The number of folds attained when crystals are formed is mainly determined by the polymer chain length, i.e. higher molecular weight PEGs will become more folded. Also, PEG can crystallise in meta-stable forms when cooled and exhibit a secondary crystallisation over time forming more stable crystals. In the case of PEG 4000 (PEG with an average molecular weight of 4000 g/mol), which has been used in this study, both the once-folded and the non-folded form can be observed after primary crystallisation but during secondary crystallisation the folded form is converted to the non-folded one. The lamellar thickness is determined by the molecular weight and the folding, i.e. a lamellar structure consisting of unfolded molecules has basically twice the thickness of one which consists of once-folded chains of the same polymer (Buckley and Kovacs, 1976).

The poor storage stability of PEG solid dispersions is well documented (Dordunoo et al., 1997; Smikalla and Urbanetz, 2007; Saers et al., 1993; Serajuddin, 1999; Bartsch and Griesser, 2004) but the role of PEG unfolding for the physical stability is not yet fully understood. It has previously been suggested that when polysorbate 80 (Morris et al., 1992) and Capmul PG8-CremophorEL (Li et al., 2009) is added to PEG they are incorporated into the amorphous domains of the polymer. Further, one of our own publications (Mahlin et al., 2004) on a study of solid mixtures of PEG and the polar lipid monoolein revealed that the lipid was intercalated into the amorphous domains of the semi-crystalline lamellar stacks of the PEG. If added components are incorporated in the amorphous regions a secondary crystallisation should promote component separation. We recently published supportive data for such transformations to take place in solid dispersions of monoolein in PEG (Mahlin et al., 2005). On the contrary, Verheyen et al. (2004) have reported that unfolding of PEG 6000 during storage did not influence the re-crystallisation and release of incorporated drugs.

The stability of solid dispersion thus seems to be highly dependent on the way components mix during preparation and the mixing behaviour is dependent on what components are included. To further understand this we have in this study investigated the addition of twelve different lipids to PEG 4000 as a model system to elucidate what properties of incorporated lipophilic components are important for the phase behaviour of the solid dispersions. The lipids are structurally related but differ in physicochemical properties such as molecular weight, lipophilicity and melting point. To get an un-biased selection of lipid properties that govern the lipid–polymer mixture behaviour we used multivariate modelling to identify important parameters for further discussion.

2. Materials

The PEG 4000 (average molecular weight 4000 g/mol; interval: 3500–4500 g/mol) was of a pharmaceutical grade and was purchased from Fluka. All lipids were purchased from Sigma–Aldrich (Germany) except Phytantriol and Selachylalcohol which were gifts from Kuraray (Japan). All lipids had a purity of at least 97%.

3. Methods

3.1. Sample preparation

Samples were prepared to consist of 25% (w/w) of the different lipids and of 75% (w/w) PEG 4000 by weighing accurate amounts of the two components into Eppendorf test tubes. The contents were melted at 100 °C and kept at that temperature for 20 min under intermittent mixing. A homogenous melt was formed in all samples, as deemed by visual inspection, and was solidified at room temperature.

3.2. Differential scanning calorimetry

The DSC analysis was performed using a Perkin Elmer DSC 7 with an Intracooler 1P add-on (Perkin Elmer, Waltham, MA, USA). Samples were weighed into 25 μl aluminium DSC pans (Perkin Elmer), heated to 100 °C, cooled to 20 °C and then stored pending analysis. This procedure was used to achieve a good contact between the sample and the pan, thereby improving the quality of the thermograms. DSC analysis was performed after 24 h and after 1 month of storage. On both occasions the following temperature program was used: (20–100–20–100–0–100) °C, the scan speed was 5 °C/min and at each maximum or minimum the temperature was kept constant for 1 min. The second heating was to get data for a freshly prepared sample ($t = 0$). The melting and crystallisation temperatures of the lipids were determined by scanning appropriate intervals for each lipid at 5 °C/min. Pure PEG 4000 was examined using the same protocol as for the mixtures and for the pure lipids the program (0–100–(−30)) °C was used.

3.3. Small angle X-ray diffraction

Small angle X-ray diffraction (SAXD) analysis was performed on beamline I711 at the synchrotron facility Maxlab (Lund University, Lund, Sweden) (Cerenius et al., 2000). The radiation wavelength was 0.1125 nm, scattering was recorded under vacuum at room temperature using a marccd 165 2D detector (Marresearch, Norderstedt, Germany). The exposure time was 300 s for each sample. The resulting CCD images were integrated to obtain 1D diffractograms using Fit2D software provided by Hammersley (2007).

The repeating period of the lamellar structures was calculated from the position of the first peak in Lorenz-corrected SAXD data using Bragg's law:

$$n\lambda = 2d \sin\theta \quad (1)$$

where n is an integer, λ is the X-ray wavelength, d is the distance between diffracting planes and θ is the scattering angle.

3.4. Principal component analysis

Principal component analysis (PCA), as implemented in Simca-P version 11.5 (Umetrics, Umeå, Sweden) was used to study similarities between different lipids with regard to the experimentally determined parameters, including crystallisation and melting parameters from DSC and lamellar thicknesses from SAXD. In PCA, many original variables are projected onto a low-dimensional coordinate system of latent variables or principal components. Lipids with similar values in the principal components thus have similar overall effects on the measured properties of the lipid–polymer mixtures.

3.5. Multivariate modelling

Molecular structures obtained from SciFinder Scholar 2006 (American Chemical Society, Washington, DC) were used as the input for 3D structure generation using Corina version 3.0 (Molecular Networks, Erlangen, Germany) (Fig. 1). A total of 669 molecular descriptors, representing mainly the molecular size, flexibility, connectivity, polarity, charge, and hydrogen bonding potential of the molecules, were calculated from the 3D structures using DragonX version 3.0 (Talete, Milan,

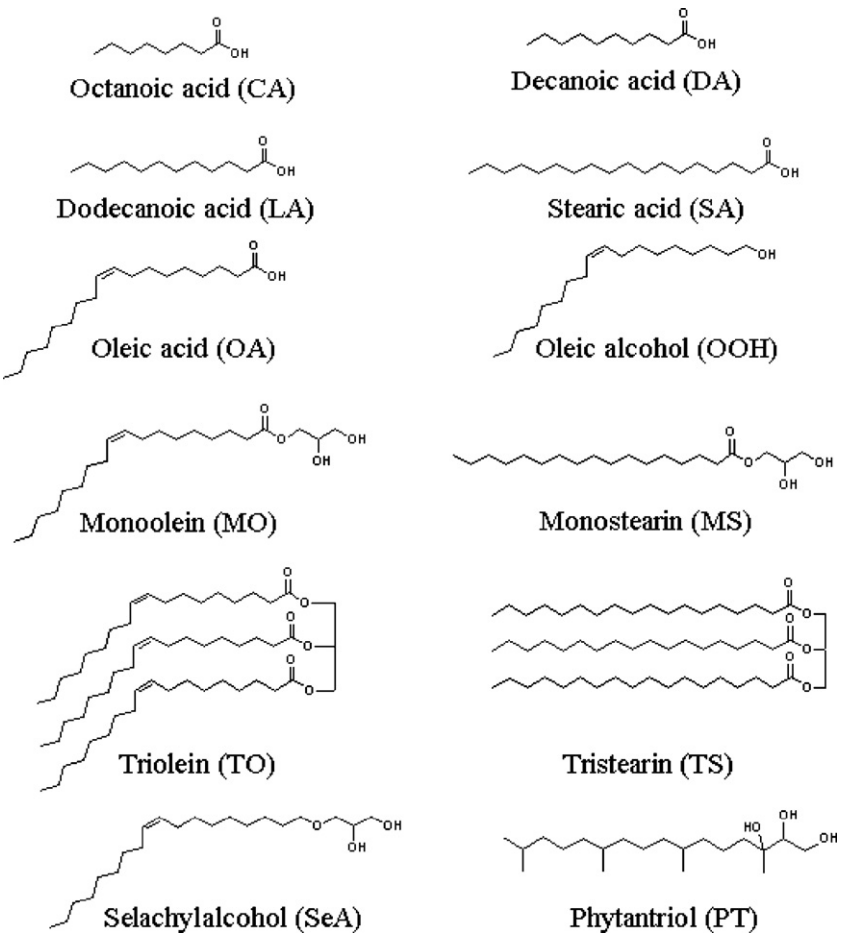

Fig. 1. Molecular structures of the lipids.

Italy) and ADMETPredictor version 1.2.4 (SimulationsPlus, Lancaster, CA, USA). The static free molecular surface areas for each different atom type were calculated using the software MAREA version 3.02, as described previously (Palm et al., 1997; Matsson et al., 2005). After removal of molecular descriptors with zero variance within the dataset, 240 descriptors were used as a starting point for the model development.

Partial least squares (PLS) modelling, as implemented in Simca-P version 11.5 (Umetrics, Umeå, Sweden), was used to derive multivariate models describing structural features that influence the fraction of folded PEG at $t = 0$ and the unfolding rates from 0 to 1 and 0 to 30 days of storage of the lipid–polymer mixtures. The number of PLS components computed was determined using Q^2, the leave-n-out cross-validated R^2, using seven cross-validation rounds. Only PLS components resulting in a positive Q^2 were computed, and the number of principal components was never allowed to exceed one-third of the number of observations used in the model. The models were refined through stepwise removal of molecular descriptors with insignificant influence. Initially, all descriptors were included in the PLS model. After the first round, the descriptors with the lowest influence on the prediction were deleted, and a new PLS model was calculated. If the exclusion of the least important descriptors resulted in a more predictive model (as assessed by a higher Q^2), the descriptors were permanently left out of the model. This procedure was repeated until no further improvement of the model could be achieved.

The root-mean-square error (RMSE) of prediction was used as a measure of the predictivity of the PLS models:

$$\mathrm{RMSE} = \sqrt{\frac{1}{n-1-p}\sum_{i=1}^{n}(y_{i,\mathrm{predicted}} - y_{i,\mathrm{measured}})^2} \quad (2)$$

where n is the number of observations, p is the number of latent variables in the PLS model, and y_{measured} and $y_{\mathrm{predicted}}$ are the experimentally determined and predicted values of the response parameter, respectively.

4. Results

All samples appeared as clear one-phase liquids in the melted state showing that the melted lipids form solutions together with the PEG. The solubility for all lipids in melted PEG is thus above 25% (w/w) at 100 °C.

4.1. Differential scanning calorimetry

4.1.1. Thermal behaviour of pure lipids

DSC measurements showed melting upon heating and crystallisation when cooled, for most of the pure lipids in the standard DSC set-up (see Table 1). Triolein (TO) did not crystallise during the standard cooling run, but crystallisation was achieved by repeated slow heating and cooling in a narrow temperature range around −5 °C. Phytantriol (PT) and Selachylalcohol (SeA) showed endothermic peaks at the temperatures given in Table 1, but deeming from the very small enthalpy of the event it was probably not melting of a fully crystallised lipid but rather of a more disordered polymorph.

Table 1
Molecular weights (M_W) of the lipids and melting and crystallisation temperatures ($T_{m,peak}$, $T_{c,peak}$) and heat of melting (ΔH_m) for the pure lipids.

Lipid	M_W (g/mol)	$T_{m,peak}$ (°C)	ΔH_m (J)	$T_{c,peak}$ (°C)
Octanoic acid	144.2	16.3	135.8	5.4
Decanoic acid	172.3	32.3	155.0	26.1
Dodecanoic acid	200.3	45.1	180.2	38.4
Stearic acid	284.5	69.8	208.0	65.0
Oleic acid	282.5	13.4	133.1	1.0
Oleic alcohol	268.5	8.6	141.0	−10.2
Monoolein	356.5	36.2	145.7	5.9
Monostearin	358.6	80.9	211.7	70.9
Triolein	885.4	4.3	126.9	−5.0**
Tristearin	891.5	73.0	216.4	49.8
Selachylalcohol	342.6	5.6*	1.9*	−5.1
Phytantriol	330.6	27.4*	21.8*	16.9

Numbers denoted with * are measured on peaks of non-regular melting and ** measured on MO which crystallised under non-standard cooling conditions.

4.1.2. Thermal behaviour of PEG–lipid mixtures

The DSC measurements on the lipid–PEG mixtures were performed after three different storage times; $t = 0$ (taken from the thermogram recorded immediately upon cooling to 20 °C), $t = 1$ and 30 days (Fig. 2). All thermograms showed melting of at least one form of PEG and, in the cases of mixtures with SA, MS and TS, lipid melting could also be detected. The two peaks which arise from PEG melting reflect the melting of the once-folded and non-folded form of PEG 4000 (Buckley and Kovacs, 1976). The pattern of the PEG melting was affected by the addition of the lipid in all samples, which can be seen in the thermograms in all measurements in primarily two ways: (i) the melting points are decreased and (ii) the area ratio between the peaks for the folded and non-folded forms change compared to pure PEG. Further, the qualitative appearances of the peaks changed for many samples (Fig. 2). In all samples melting temperatures for the folded and the non-folded forms of PEG were determined. In all of the mixtures the temperature of both PEG melting peaks was decreased to the same extent compared to the corresponding melting temperatures of pure PEG. Therefore only one melting temperature is given in Table 2, that of the non-folded form at $t = 1$. Thus, these values represent ability of the lipids to depress the melting temperature of the PEG.

Thermal events during cooling were also recorded. They revealed PEG crystallisation in all samples on cooling to 20 °C and, in three cases (SA, MS and TS), separate crystallisation of the lipid was observed. The crystallisation peak for PEG observed during cooling will be referred to as the primary crystallisation. Its onset temperature, i.e. the crystallisation temperature (T_c), was decreased to varying extents by all lipids (see Table 2), as compared to pure PEG which crystallised at 45.4 °C. All T_c observed upon repeated heating and cooling of a specific sample were within 0.5 °C.

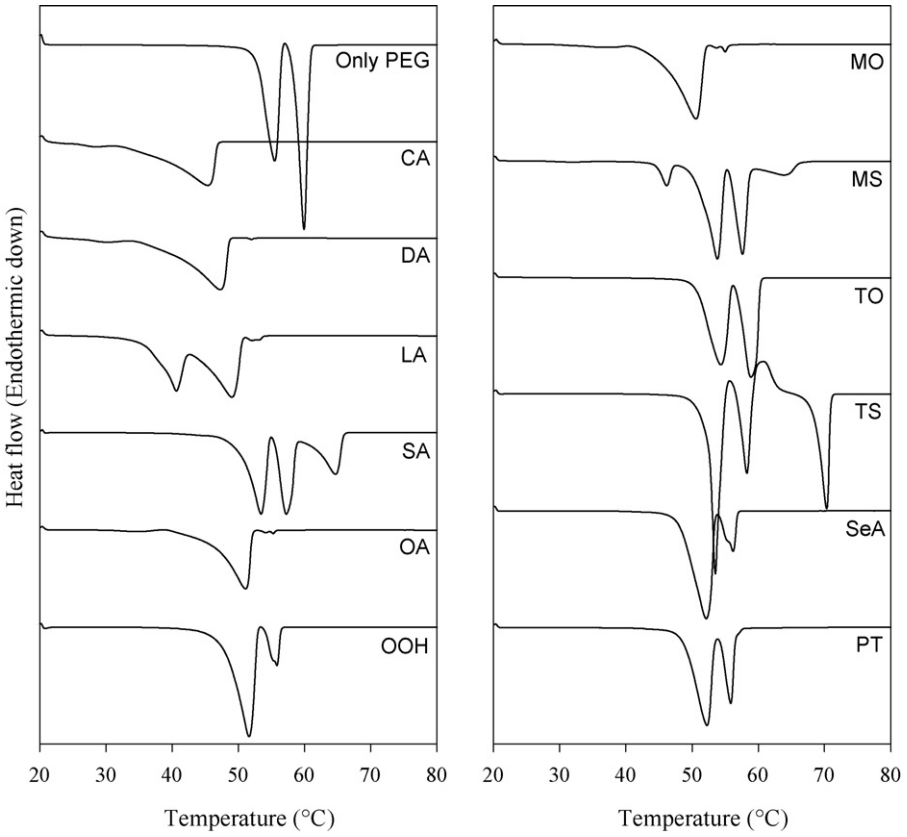

Fig. 2. Weight-normalized DSC thermograms of pure PEG and the lipid–PEG samples (denoted by the lipid abbreviations, see Fig. 1) at $t = 0$. PEG melting peaks were observed in all samples. For SA, TS and MS, additional endothermic peaks were observed, related to the melting of the lipid and for TS there was also an exothermic event interpreted as crystallisation of lipid that was released when the PEG melted.

Table 2
Experimental data for the PEG–lipid mixtures.

Lipid	$T_{c,PEG}$ (°C)	$T_{m,PEG}$ (°C)	$f_{f,t=0}$	$R_{u,0-1}$ (day^{-1})	$R_{u,0-30}$ (day^{-1})	$d_{t=1}$ (nm)	$d_{t=30}$ (nm)
Octanoic acid	29.7	49.4	1	0.065	0.019	18.1	19.0/27.4
Decanoic acid	30.9	50.7	0.99	0.040	0.0093	15.0	14.2
Dodecanoic acid	33.5	53.7	0.96	0.26	0.020	13.1	13.1
Stearic acid	30.1	56.6	0.62	0.067	0.0069	13.0	12.8
Oleic acid	24.6	54.1	0.98	0.083	0.014	16.3	19.0
Oleic alcohol	39.1	55.4	0.85	0.24	0.019	13.2	13.1
Monoolein	34.0	53.5	0.97	0.080	0.0096	15.8	15.9
Monostearin	38.4	57.0	0.63	0.075	0.011	13.1	12.8
Triolein	42.3	58.9	0.57	0.22	0.0069	13.4	12.6/14.4
Tristearin	41.3	57.7	0.67	0.076	-0.0012	13.1	13.0/14.8
Selachylalcohol	39.2	55.7	0.83	0.13	0.014	13.1	13.3
Phytantriol	34.7	55.7	0.73	0.085	0.0036	13.3	13.2

$T_{c,PEG}$ is the crystallisation temperatures for the PEG from DSC, $T_{m,PEG}$ is the melting temperature of non-folded PEG at $t = 1$ day, f_f is the fraction folded PEG at $t = 0$, $R_{u,0-1}$ and $R_{u,0-30}$ are the PEG unfolding rates from 0 to 1 day and 0 to 30 days, respectively, and $d_{t=1}$ and $d_{t=30}$ are the PEG lamellar thicknesses at days 1 and 30.

In order to estimate the fraction of the crystallised PEG that was present in the folded form, the DSC data was further analyzed. The fraction of folded PEG (f_f) was estimated as

$$f_f = \frac{A_{folded}}{A_{folded} + A_{unfolded}} \quad (3)$$

where the areas under melting peaks (A) for the two PEG forms were determined from the DSC thermograms. Due to poor separation of the peaks, A was calculated from non-linear regression of split Pearson VII type peaks to the heat flow signal of the thermograms around the melting peaks. The fitting of the theoretical peak to data was good, with goodness of fit values (R^2) ranging from 0.96 to 0.99.

At $t = 0$, directly after primary crystallisation, the melting peaks from the folded and non-folded forms of PEG were approximately equal in size in pure PEG ($f_f = 0.48$). In the PEG–lipid samples the folded form dominated in all samples (f_f values ranging from 0.57 to 1), denoting that the lipids promote formation of the folded form of PEG. The smallest effect was seen in the TO mixture, where the fraction folded was 0.57, and the largest in the mixtures with CA and DA, where virtually only the folded form was detected (see Table 2). Due to secondary crystallisation the proportion of folded polymer had decreased after 1 day and even more so after 30 days of storage in all samples except TO and TS, where the f_f was approximately constant or even increased slightly. An example of typical behaviour with unfolding over time is shown in Fig. 3 for the CA–PEG mixture.

In the thermograms of the TS–PEG mixture a small exothermic peak was observed, coinciding with the melting of the PEG, which was interpreted as crystallisation of lipid (Fig. 2). As shown previously for MO (Mahlin et al., 2004, 2005) and most likely for all other lipids, it becomes incorporated to some degree into the PEG-rich phase during crystallisation of the mixture. Hence, when TS was released upon PEG melting, it is given the opportunity to crystallise. The only other lipids that have high enough melting points to crystallise upon melting of the PEG were MS and SA. However, the absence of a lipid crystallisation peak for these lipids in mixtures with PEG does not mean that they were not incorporated in the polymer; rather, they may have a smaller driving force for nucleation, i.e. crystallisation will not occur during the timescale of the experiment.

The rate at which the unfolding process occurred (R_u) was calculated as the proportion of the folded polymer that was transformed over a certain time period:

$$R_u = \frac{f_{f,t=0} - f_{f,t=i}}{f_{f,t=0}(t_i - t_0)} \quad (4)$$

where $f_{f,t=0}$ and $f_{f,t=i}$ are the estimated fractions of folded PEG at the start and end of the interval, respectively, and t_i and t_0 are the end and start time points of the interval. The unfolding rate was calculated for the initial period (0–1 day) and for the whole study (0–30 days); the rates are listed in Table 2. The unfolding rate during the first day was in most cases more than 10-fold that of the longer period. The fastest unfolding initially was seen in mixtures with LA ($R_u = 0.26$ days^{-1}), OOH (0.24 days^{-1}) and TO (0.22 days^{-1}). LA (0.020 days^{-1}) and OOH (0.019 days^{-1}) also had the highest rate over the longer period together with CA (0.019 days^{-1}) whereas unfolding in the TO (0.0069 days^{-1}) and TS (−0.0012 days^{-1}) samples slowed down considerably after the initial phase. The lowest rate was seen for the TS sample in which a modest unfolding was recorded initially (0.076 days^{-1}) but none or even slightly negative (−0.0012 days^{-1}) over the longer period. It appears as if the TS–PEG and TO–PEG mixtures settle during the first 24 h, i.e. after primary crystallisation, into a stable or highly stabilized state with a large proportion of folded PEG.

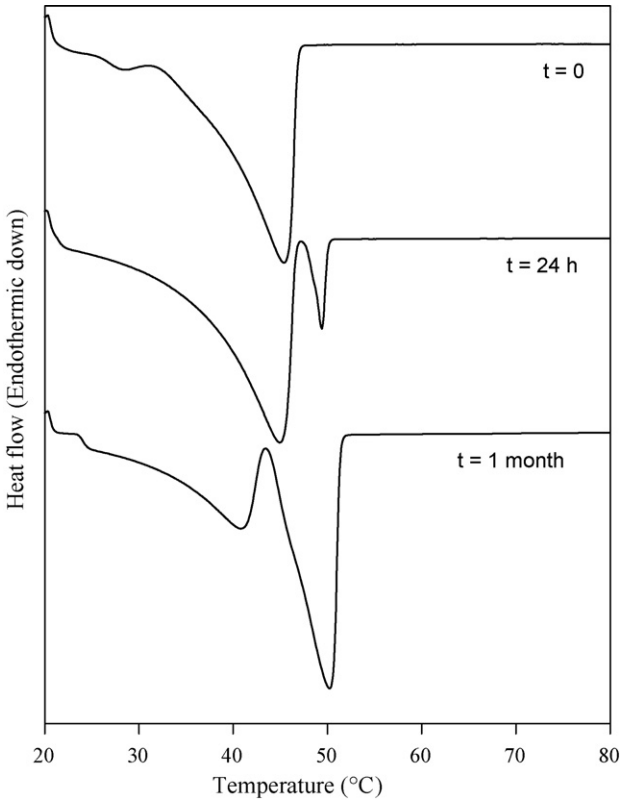

Fig. 3. Thermograms of the CA–PEG sample after different periods of storage ($t = 0$, $t = 24$ h and $t = 1$ month). During storage, the non-folded form (the higher melting peak at approximately 50 °C) increased as the folded form (lower melting point) decreased.

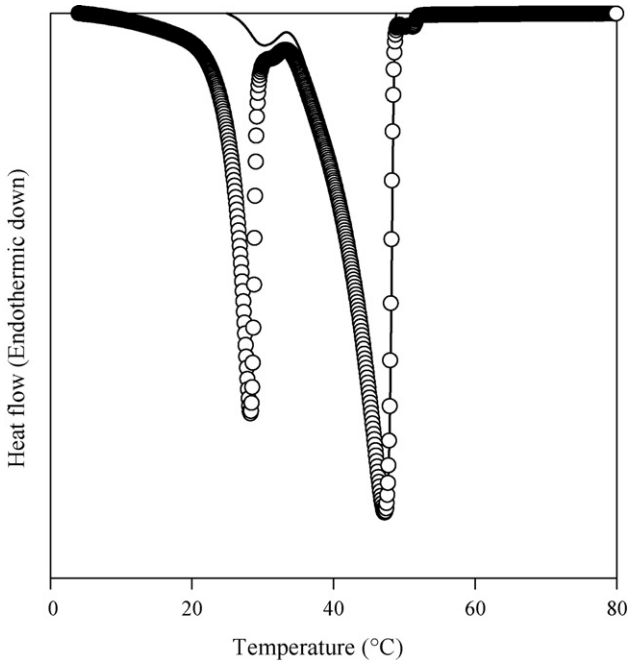

Fig. 4. Thermograms from heating the DA–PEG from 20 °C (line) and from 0 °C (rings) showing virtually identical PEG melting peaks. The peak at 27 °C is from melting of the lipid.

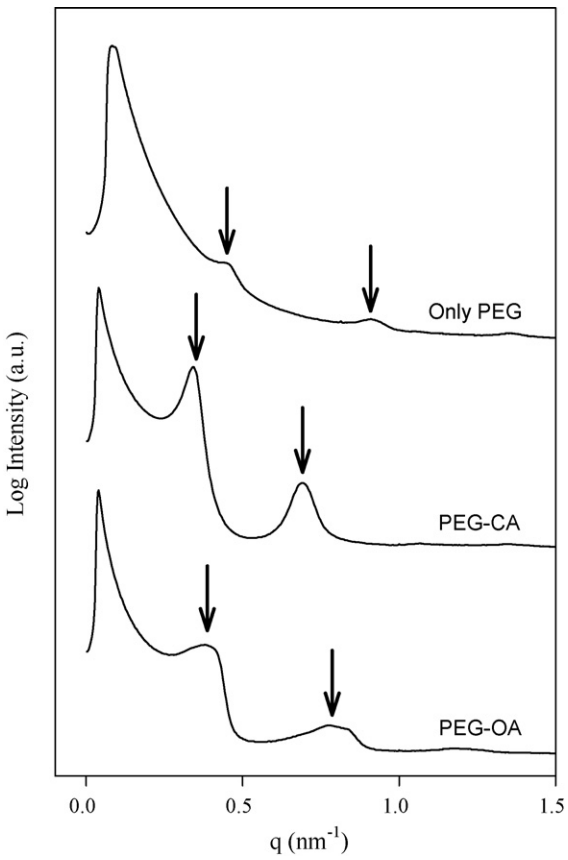

Fig. 5. Examples of diffractograms at $t = 1$ day. The arrows show the first and second diffraction peaks in each sample. Diffraction from pure PEG shows a lamellar structure with $d = 13.7$ nm, CA–PEG diffracts more strongly and has a lamellar distance of 18.1 nm and the OA–PEG shows broader peaks indicating a larger distribution in repeat distances around $d = 16.3$ nm. The diffractograms have been separated by an appropriate integer for clarity.

To evaluate the effect of crystallisation of the lipid on PEG crystallisation the samples were cooled to 0 °C and then immediately reheated to 100 °C. CA was the only lipid that crystallised when cooled to 0 °C but not when cooled to 20 °C. The melting peaks of PEG in mixture with CA were virtually identical after cooling to either of the two temperatures (Fig. 4). Thus, the crystallisation and melting of the CA seem not to affect the PEG folding behaviour. In the DA–PEG mixture, a small melting peak from non-folded PEG was observed after cooling to 0 °C but not when cooled to 20 °C, which probably is a result of the longer time at temperatures where crystallisation of the PEG can take place, before the melting occurs. In the pure PEG sample a slight increase of the non-folded form could be seen after cooling to 0 °C compared to cooling to 20 °C (data not shown) which supports this assumption. Taken together, this indicates that the physical form of the lipid in the crystallised mixture has no effect on the melting pattern of PEG and, hence, the folding behaviour of the polymer.

In most thermograms, a small endothermic event was visible as a first stage in the PEG melting (see Fig. 4). The origin of this is unknown but may reflect the presence of a higher degree of folding in the sample, e.g. if there is a small amount of twice folded PEG present in a sample otherwise dominated by the once-folded. However, the contribution of this peak to the overall heat of melting is negligible, and it is therefore excluded from further discussion in present work.

4.1.3. Small angle X-ray diffraction

Bragg peaks originating from the lamellar structure of PEG were observed in all SAXD diffractograms (examples in Fig. 5). The addition of a lipid, as well as the storage time, affected the appearance of the diffractograms. The diffraction pattern from pure PEG 4000 after 1 day of storage showed only one set of diffraction peaks, the primary peak at $q = 0.46\ \text{nm}^{-1}$ and the secondary at $q = 0.92\ \text{nm}^{-1}$, corresponding to a lamellar distance of 13.7 nm which is slightly larger than would be expected theoretically for the once-folded form of the polymer chain (12.33 nm; Buckley and Kovacs, 1976) but similar to Cheng et al. (1991) who reported a lamellae thickness of 13.7 nm for a batch with a molecular weight of 4250 g/mol. During storage another peak appeared at $0.38\ \text{nm}^{-1}$ ($d = 16.4$ nm). That peak is probably the result of non-integral folding of the PEG chains, which has been reported previously (Cheng et al., 1990, 1991). The stable, non-folded, form of the PEG did not give rise to any detectable peaks in the measurements except in the CA sample; see below. The reason for the absence of diffraction peaks has been discussed earlier (Mahlin et al., 2004, 2005) and is due to the fact that virtually no amorphous domains are present in the non-folded PEG structure, resulting in a lack of the periodic electron density differences that are the prerequisites for diffraction.

The appearance of the PEG diffraction peaks changed when different lipids were added. Some mixtures gave rise to sharp peaks indicating a highly ordered structure and some gave broader peaks due to a wider distribution of repeat distances (compare CA and OA in Fig. 5). In the CA, TS and TO samples a second set of diffraction peaks from PEG appeared in the 30 days samples that were not visible after 1 day. In the case of the CA sample, the 1 day diffractogram displayed a lamellar structure with thickness 18.1 nm. After 30 days, what probably was the same structure remained ($d = 19.0$ nm) but also a second lamellar structure with $d = 27.4$ nm appeared (Fig. 6). The second structure is presumably non-folded PEG, since it has twice the thickness of the once-folded pure PEG. In the case of TS and TO samples, peaks were detected at $t = 1$ day that represent lamellar thicknesses of 13.1 and 13.4 nm, respectively. After 30 days double peaks with d-values of 13.0 and 14.8 nm for TS and 12.7 and 14.4 nm for TO, were observed.

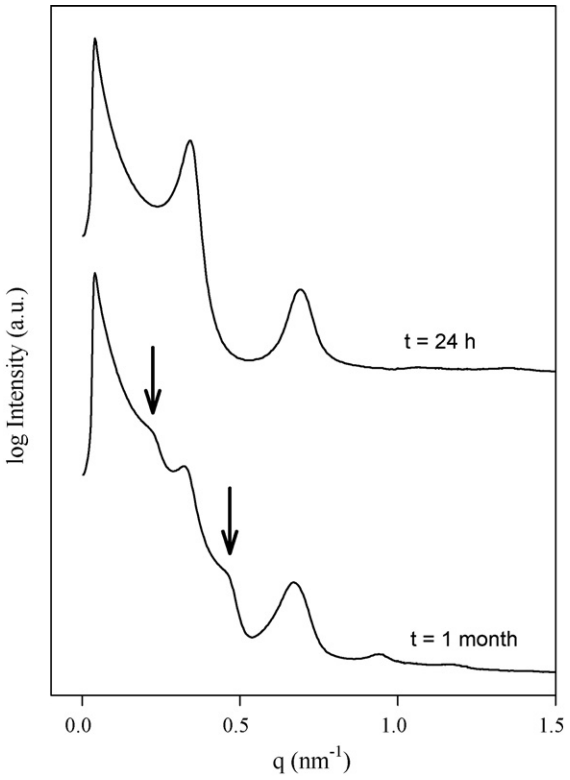

Fig. 6. Diffractograms of the CA–PEG sample at $t = 1$ and 30 days. After 1 day only one lamellar structure was detectable, giving the peaks at $q = 0.35$ and 0.70 nm^{-1}. After 30 days that structure remained, although at slightly lower q, and there were also peaks from a second lamellar phase marked with arrows at $q = 0.23$ and 0.46 nm^{-1}. The diffractograms have been separated by an appropriate integer for clarity.

Most lipids in the solid state can also diffract in the small angle region as a result of having lamellar crystal structures (Larsson, 1994). All lipids with melting points above 20 °C showed sharp diffraction peaks at specific q (or θ) values depending on the molecular structure, showing that crystals of lipid were present in the samples (data not shown). The lipids with melting points below 20 °C did not diffract in the tested q-range indicating that they did not form lamellar crystals in mixtures with PEG. PT and SeA gave broad peaks at $q = 2.39$ and 2.16 nm^{-1}, respectively, indicating an ordering which is probably due to orientation of the molecules into a lamellae-like structure in which the polar–apolar separation is less distinct than that in lamellar solid crystals of the other lipids. Hence, both DSC and SAXD data indicates that the SeA and PT lipids form more disordered crystal polymorphs than the other lipids that crystallise at room temperature in mixtures with PEG 4000.

4.1.4. Principal component analysis

Principal component analysis (PCA) was used to aid in the interpretation of the experimental data for the lipid–PEG mixtures. The PCA was based on experimentally determined parameters for the lipid–PEG mixtures: PEG melting points, fraction folded, unfolding rates and lamellar thicknesses. The resulting scatter plot of the two most important principal components ($t[1]$ and $t[2]$) is shown in Fig. 7. The lipids could be divided into three groups. Group 1 (consisting of MO, OA, CA and DA) was clearly separated from the rest of the lipids along the first principal component, and group 2 (SA, MS, TO, SeA, PT and TS) was separated from the two remaining lipids (LA and OOH; group 3) along the second principal component. Comparison of the groups reveals that group 1 differs from the other two primarily by having a larger degree of folded PEG (in excess of 0.95 at $t = 0$) and large lamellar distances. The lipids in group 2 are characterised by low to moderate PEG folding, high PEG melting points

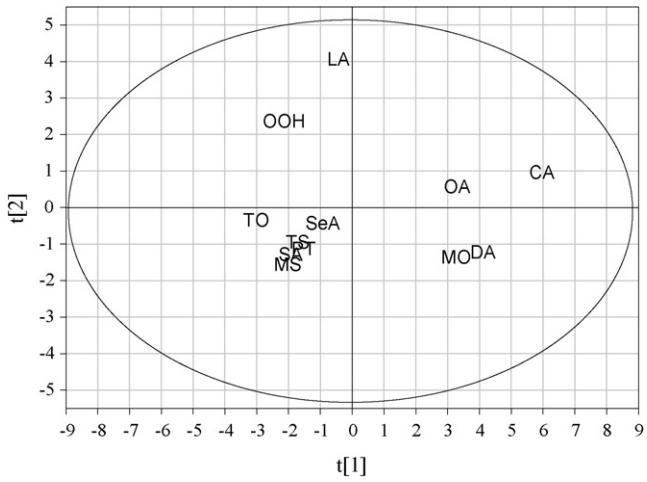

Fig. 7. Score scatter plot from the principal component analysis based on experimental data for the lipid–PEG mixtures. Each point is denoted with the lipid abbreviation. The first two principal components ($t[1]$ and $t[2]$) explain 49% and 18% of the variance in the measured parameters, respectively.

and slow unfolding. The lipids in group 3 differ from those in group 2 primarily by exhibiting much higher unfolding rates.

4.1.5. Lipid properties that influence the fraction of folded PEG and the rate of unfolding

Partial least squares (PLS) modelling was used to correlate experimentally determined properties of the mixtures (f_f at $t = 0$ and the R_u for 0–1 and 0–30 days) to molecular descriptors and physical properties for the pure lipids. Separate models were developed for each of the three properties of the mixtures. For the fraction of folded PEG, 79% of the variance was explained by the model (Fig. 8). This is comparable to similar models of e.g. aqueous solubility of drugs (Parshad et al., 2002). After excluding variables

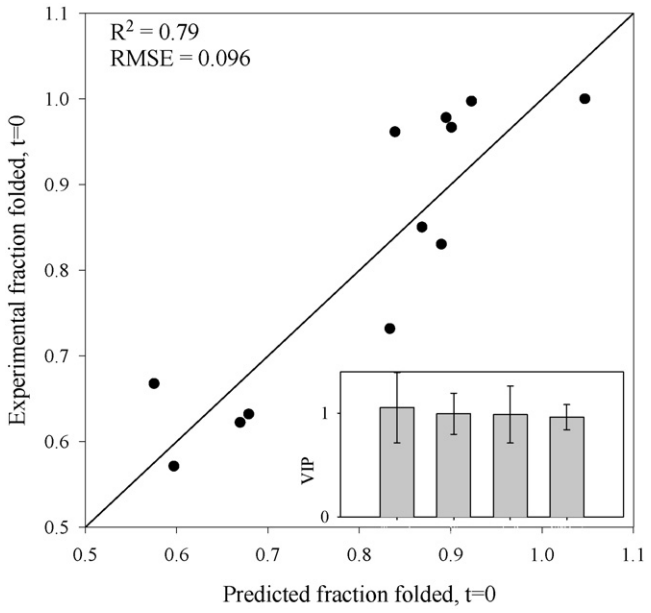

Fig. 8. Experimentally observed folded fractions at $t = 0$ compared to values predicted by the PLS model. Each point represents one of the lipids. The unity line is shown for visual guidance. Embedded: variable importance (VIP) plot displaying the relative importance of the molecular descriptors in the model. From left to right: T_c, peak: the crystallisation point of the pure lipids; X_t: the total structure connectivity index; log P: the octanol–water partition coefficient; NPSA$_{sat}$: the relative contribution of saturated non-polar atoms to the molecule surface area. The error bars denote the standard errors calculated from the seven cross-validation rounds.

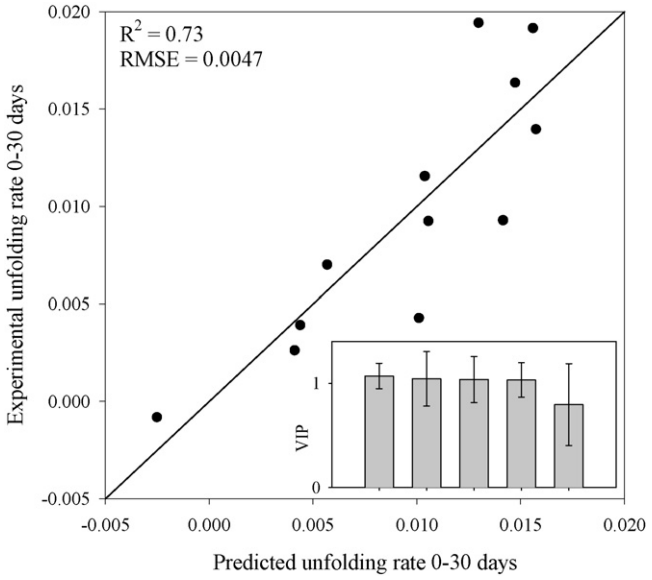

Fig. 9. Experimentally observed unfolding rates 0–30 days compared to values predicted by the PLS model. Each point represents one of the lipids. The unity line is shown for visual guidance. Embedded: variable importance (VIP) plot displaying the relative importance of the molecular descriptors in the model. From left to right: MSD: the mean square distance index; BoxZ 3D: the largest dimension of the tightest enclosing box; RgGrav 3D: the gravitational radius of gyration; TPSA: the total polar surface area; $NPSA_{unsat}$, the relative contribution of unsaturated non-polar atoms to the molecule surface area. The error bars denote the standard errors calculated from the seven cross-validation rounds.

having a small influence on f_f, four molecular descriptors were left in the final model: the crystallisation temperature of the pure lipids ($T_{c,peak}$); the total structure connectivity index (X_t), which increases with the number of carbon atoms in a molecule and the number of carbon–carbon bonds, thereby reflecting the molecule size and the degree of branching; the calculated octanol–water partition coefficient ($\log P$); and the relative molecular surface area contributed by saturated non-polar atoms (%$NPSA_{sat}$). All descriptors had a similar influence on the model, as shown by the variable importance (VIP) parameter (Fig. 8; inset).

The statistics were lower ($R^2 = 0.64$) for the PLS model of the unfolding rate 0–1 day, which limits the possibility of drawing reliable conclusions of the lipid characteristics underlying the differences in this property. A larger fraction of the variation was explained by the model of the unfolding rate 0–30 days ($R^2 = 0.73$ and $Q^2 = 0.64$; Fig. 9). Thus, subsequent analyses were focused on this model. After excluding insignificant molecular descriptors, the final model consisted of five descriptors: the mean square distance index (MSD), which is a topological index that increases with increasing branching of the molecule; the largest dimension of the tightest enclosing box (BoxZ 3D) and the gravitational radius of gyration (RgGrav 3D), which both describe the three-dimensional shape of the lipid; the total surface area of polar atoms (TPSA); and the relative molecular surface area contributed by unsaturated non-polar atoms (%$NPSA_{unsat}$). The plot of observed versus predicted unfolding rates and the VIP plot are shown in Fig. 9.

5. Discussion

5.1. Formation of the PEG structure

This study aimed at finding properties of the lipids that have influence on the crystallisation behaviour and, hence, the solid state structure of the PEG. Therefore, unique features of some of the lipids will first be discussed and then the more general patterns.

All lipids formed one-phase systems with PEG 4000 in the melted state and crystallised into a PEG-rich phase and a lipid phase on cooling at room temperature. Three of the lipids crystallised separately at a higher temperature than PEG, i.e. before primary crystallisation of the polymer. We found no indication of that such early stage phase separation would have an impact on the crystallisation of the PEG-rich phase. As it was seen in the DA case (Fig. 4), the crystallisation of the lipids which occurred after the primary crystallisation of PEG did not seem to affect the PEG folding pattern to a notable extent either. The presence of a solid lipid, compared to the presence of a melted one within the PEG structure may be of significance over longer time periods i.e. during secondary crystallisation. However, we found no pattern in the differences in the PEG structure at 30 days between the samples which had crystalline lipid phase and those who had a liquid lipid phase.

The PCA revealed three groups of lipid–PEG mixtures, of which the lipid–PEG mixtures in group 1 differed to a greater extent from the rest of the mixtures. Most notably, the lamellar thicknesses in group 1 were larger than for the rest of the lipids, indicating that the lipids were incorporated to a higher degree in the lamellae. In groups 2 and 3 the lamellar thicknesses were very close to that of the pure PEG sample suggesting that no or very little lipid had been incorporated. If all the lipid would be intercalated into the lamellar structure, assuming equal density for the lipid and polymer and that the basic structure of PEG remains unaltered with the lipids present (i.e., either folded or non-folded), 75% of the thickness of the lamellae would be related to PEG and the total thickness would be 13.7 nm/0.75 = 18.3 nm. The lipids have slightly lower densities than the polymer but the values of 18–19 nm measured for CA and OA still indicate very high degrees of inclusion of the lipid into the polymer structure for these two lipids.

Interestingly, the CA–PEG mixture differed from the pure PEG samples and from all other PEG–lipid mixtures in that the non-folded form of PEG was detected by SAXD. We suggest that the CA induced the formation of an amorphous phase of disordered polymer chain ends, between regions of crystalline PEG, into which the lipid was intercalated during secondary crystallisation. In that way an amorphous-crystalline lamellar structure was formed with a periodicity close to the length of a fully extended polymer chain. CA is also the lipid that increased the folded PEG fraction and swells the lamellar structure the most, indicating a high degree of lipid incorporation. In conclusion, high degree of lipid incorporation in the PEG-rich phase initially, seemingly enables an intercalation of the lipid into non-folded lamellar crystals of PEG upon unfolding.

Similarly to the CA mixture, the TS and TO samples displayed two sets of diffraction peaks after 30 days at slightly lower and higher q than the one at day 1. However, in this case, a lamellar structure of folded PEG chains is the most probable cause of both diffraction peaks. A unique property of the two triglycerides is that the fraction of folded PEG increases from day 1 to day 30. It seems very unlikely that the non-folded PEG chains would fold over time, so the explanation for the increase in folded fraction can only be that inter-lamellar amorphous phase, not detectable by DSC or SAXD, transforms on secondary crystallisation to the folded form. If this process is progressing faster than the transition from the folded to the non-folded form the fraction of folded PEG will increase over time, which is also seen for mixtures with the triglycerides. Hence, a possible explanation for the appearance of two similar diffraction peaks, in this case, would be that the intercalation of lipid in the folded PEG structure, formed during secondary crystallisation, is different from the one formed during primary crystallisation.

Fig. 10 shows the folded fraction of the PEG at $t = 0$ versus the lamellar thickness of the folded form of PEG. The plot indicates that inclusion of lipid by swelling of the lamellae takes place only when essentially all PEG has attained the folded form. The plot shows that only in the PEG samples where the folded form dominates

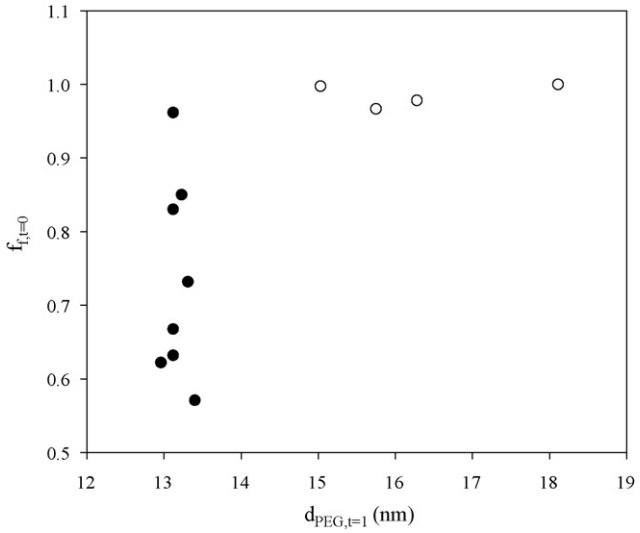

Fig. 10. The fraction of folded PEG at $t = 0$ ($f_{f,t=0}$) plotted against the PEG lamellar distance at $t = 1$ day ($d_{PEG,t=1}$) for each lipid–PEG sample. The unfilled rings are the group 1 lipids from the PCA and the filled rings are groups 2 and 3 lipids.

completely a significant swelling of the folded structure is observed. Both folding and swelling of the structure occurs during primary crystallisation and during storage the folded fraction decreased.

Eutectic and monotectic mixing behaviours has previously been reported for PEG mixtures (Craig, 2002; Huang and Nishinari, 2001). In the ideal case, the melting point depression depends on the number of moles of another component present. Since a constant weight percent of the lipid has been used here, the number of moles per kilogram mixture is different and dependent on the molecular weight of the lipid. In fact, the melting point of the non-folded PEG at $t = 1$ day was linearly correlated to the molar concentration of lipid in the sample, see Fig. 11. The deviation from a fitted line presumably indicates the interaction between the components but the exact nature of these interactions cannot be deduced from our data.

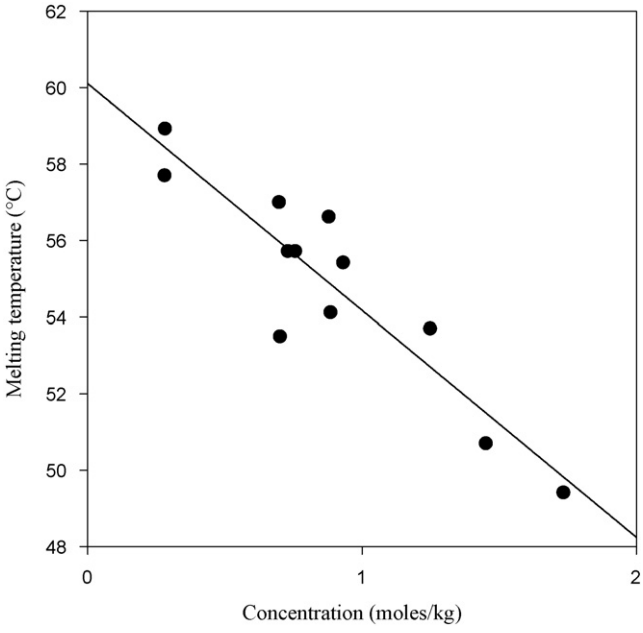

Fig. 11. PEG melting temperatures for all lipid–PEG samples ($T_{m,PEG}$) plotted against the concentration of each lipid in the samples. The line represents a linear regression ($R^2 = 0.83$).

PLS multivariate analysis was used to further characterise the influence of the lipids on the degree of folding of the PEG. In the best PLS model the number of descriptors was reduced to four: one determined experimentally ($T_{c,peak}$) and three calculated (%$NPSA_{sat}$, the structure connectivity index and log P). The model revealed that for a lipid to promote the folding of the PEG it should have a low crystallisation point, have a small proportion of non-polar surface, a low structure connectivity index and a low log P. The degree of PEG folding can be assumed to be determined by interactions between the lipid molecules and the PEG during primary crystallisation. The model reveals that for a molecule to affect the folding to a high extent it should be small and hydrophilic. Not surprising, such molecules apparently interact more strongly than more lipophilic ones with the rather hydrophilic PEG chains. The hydrophilic lipids can probably remain in a one-phase system with PEG until crystallisation, and maybe also after crystallisation, whereas the more lipophilic ones will phase separate at some point.

5.2. Rate of unfolding

The unfolding rates vary a lot between the samples, from virtually no unfolding for TS to approximately 60% of the folded form being transformed in 30 days for LA, OA and OOH. For the group 1 lipids which are incorporated to a high extent in the PEG lamellae the unfolding rates correlate to some degree with the lamellae thicknesses. This could mean that high incorporation of lipid creates more unstable systems in which the strive for unfolding is stronger, or that the presence of large amounts of lipid facilitates the unfolding process. Since unfolding occurs at markedly different rates also in those of the samples where there is no or very limited incorporation of lipid, that cannot be the whole explanation. The group 3 lipids, LA and OOH, have the highest unfolding rates of all but are not incorporated in the PEG to an appreciable extent so if the incorporated amount is a factor involved in the unfolding there are also other factors. The PLS analysis for the unfolding rate (0–30 days) showed that for a molecule to retard unfolding effectively it should ideally be large, branched and have a small proportion of polar surface area, exemplified by the triglycerides (TO and TS) and phytantriol. These are the exact opposite properties to those of the lipids that promote folding. It thus seems that molecular interactions between PEG and the more hydrophilic lipids first, during cooling, make the PEG adopt a less stable form but after cooling also allow the polymer to unfold, whereas the bulky lipophilic lipids are incorporated in the PEG structure to a limited extent but the small amount present still makes unfolding difficult. The mechanism for this is not obvious. One possibility is that the solid lipid crystals present in the dispersions somehow prevents unfolding through interfacial effects between the phase separated lipid and the hydrophilic PEG chains. Another possibility is that the crystallisation of pure lipid before crystallisation of PEG affects the PEG crystallites in such a way that unfolding is hampered. That could be due to facilitated PEG nucleation in the presence of solid material (lipid) leading to smaller PEG crystals in which flexibility and thus unfolding is restricted. The fact that TS crystallises during heating after the folded PEG has melted shows that the lipid is not all in a separate phase but is also incorporated in the PEG; this was also corroborated by the SAXD data.

6. Conclusions

Previous publications show that the presence of the lipid Monoolein promotes formation of the folded form of PEG upon crystallisation of the polymer (Mahlin et al., 2005). In this study we show that the folding depends on the physicochemical properties of lipid present. All tested lipids promoted PEG folding during initial crystallisation and slowed the unfolding kinetics. The small,

more hydrophilic, lipids promoted folding the most. Some lipids were intercalated to a high extent into the amorphous domains of the PEG lamellar structure. This was seen as a substantial swelling of the lamellae thickness and was also associated with fractions of folded PEG close to 1. When Tristearin was mixed with PEG the unfolding was almost completely prevented.

Ideally, in a drug delivery vehicle, the matrix properties should be known and constant over time. From that perspective the Tristearin–PEG system is very interesting since TS effectively prevented the unfolding process that normally occurs for PEG 4000. Other lipids such as oleic acid and decanoic acid increased the proportion of the folded PEG form which might be needed if an increased volume of amorphous PEG is desired. Unfortunately, those systems also proved very unstable with a rather fast unfolding process occurring.

The PLS analysis was shown to be useful as a tool for finding properties of the lipids that affect the solid state of PEG. The found correlations are potentially useful guides for future work on understanding the underlying mechanisms of solid dispersion structure formation. More studies are also needed to determine whether these findings can be transferred to other types of substances than lipids.

Acknowledgments

The authors would like to thank the Chalmers foundation (JU) and AstraZeneca (DM) for financial support. Yngve Cerenius and Matti Knaapila are acknowledged for their assistance during the SAXD measurements.

References

Alden, M., Tegenfeldt, J., Sjokvist, E., 1992. Structure of solid dispersions in the system polyethylene glycol-griseofulvin with additions of sodium dodecyl-sulfate. Int. J. Pharm. 83, 47–52.

Bartsch, S.E., Griesser, U.J., 2004. Physicochemical properties of the binary system glibenclamide and polyethylene glycol 4000. J. Therm. Anal. Calorim. 77, 555–569.

Buckley, C.P., Kovacs, A.J., 1975. Melting behaviour of low molecular weight (ethylene-oxide) fractions. I. Extended chain crystals. Prog. Colloid Polym. Sci. 58, 44–52.

Buckley, C.P., Kovacs, A.J., 1976. Melting behavior of low-molecular weight poly (ethylene-oxide) fractions. 2. Folded chain crystals. Colloid Polym. Sci. 254, 695–715.

Cerenius, Y., Stahl, K., Svensson, L.A., Ursby, T., Oskarsson, A., Albertsson, J., Liljas, A., 2000. The crystallography beamline I711 at MAX II. J. Synchrotron Radiat. 7, 203–208.

Cheng, S.Z.D., Zhang, A., Chen, J.H., 1990. Existence of a transient nonintegral folding lamellar crystal in a low-molecular mass poly(ethylene oxide) fraction crystallized from the melt. J. Polym. Sci. Part C: Polym. Lett. 28, 233–239.

Cheng, S.Z.D., Zhang, A.Q., Barley, J.S., Chen, J.H., Habenschuss, A., Zschack, P.R., 1991. Isothermal thickening and thinning processes in low-molecular-weight poly(ethylene oxide) fractions. 1. From nonintegral-folding to integral-folding chain crystal transitions. Macromolecules 24, 3937–3944.

Chiou, W.L., Riegelmann, S., 1971. Pharmaceutical applications of solid dispersion systems. J. Pharm. Sci. 60, 1281–1302.

Craig, D.Q.M., 2002. The mechanisms of drug release from solid dispersions in water-soluble polymers. Int. J. Pharm. 231, 131–144.

Crowley, M.M., Zhang, F., Repka, M.A., Thumma, S., Upadhye, S.B., Battu, S.K., Mcginity, J.W., Martin, C., 2007. Pharmaceutical applications of hot-melt extrusion: Part I. Drug Dev. Ind. Pharm. 33, 909–926.

Dordunoo, S.K., Ford, J.L., Rubinstein, M.H., 1997. Physical stability of solid dispersions containing triamterene or temazepam in polyethylene glycols. J. Pharm. Pharmacol. 49, 390–396.

Hammersley, A., 2007. The Fit2D Home Page.

Huang, L., Nishinari, K., 2001. Interaction between poly(ethylene glycol) and water as studied by differential scanning calorimetry. J. Polym. Sci. Part B: Polym. Phys. 39, 496–506.

Larsson, K., 1994. Lipids: Molecular Organization, Physical Functions and Technical Applications. Oily Press Lipid Library.

Leuner, C., Dressman, J., 2000. Improving drug solubility for oral delivery using solid dispersions. Eur. J. Pharm. Biopharm. 50, 47–60.

Li, P., Hynes, S.R., Haefele, T.F., Pudipeddi, M., Royce, A.E., Serajuddin, A.T.M., 2009. Development of clinical dosage forms for a poorly water-soluble drug. II. Formulation and characterization of a novel solid microemulsion preconcentrate system for oral delivery of a poorly water-soluble drug. J. Pharm. Sci. 98, 1750–1764.

Mahlin, D., Ridell, A., Frenning, G., Engstrom, S., 2004. Solid-state characterization of PEG 4000/monoolein mixtures. Macromolecules 37, 2665–2667.

Mahlin, D., Unga, J., Ridell, A., Frenning, G., Engstrom, S., 2005. Influence of polymer molecular weight on the solid-state structure of PEG/monoolein mixtures. Polymer 46, 12210–12217.

Matsson, P., Bergstrom, C.A.S., Nagahara, N., Tavelin, S., Norinder, U., Artursson, P., 2005. Exploring the role of different drug transport routes in permeability screening. J. Med. Chem. 48, 604–613.

Morris, K.R., Knipp, G.T., Serajuddin, A.T.M., 1992. Structural-properties of polyethylene-glycol polysorbate-80 mixture, a solid dispersion vehicle. J. Pharm. Sci. 81, 1185–1188.

Nakamichi, K., Nakano, T., Yasuura, H., Izumi, S., Kawashima, Y., 2002. The role of the kneading paddle and the effects of screw revolution speed and water content on the preparation of solid dispersions using a twin-screw extruder. Int. J. Pharm. 241, 203–211.

Palm, K., Stenberg, P., Luthman, K., Artursson, P., 1997. Polar molecular surface properties predict the intestinal absorption of drugs in humans. Pharm. Res. 14, 568–571.

Parshad, H., Frydenvang, K., Liljefors, T., Larsen, C.S., 2002. Correlation of aqueous solubility of salts of benzylamine with experimentally and theoretically derived parameters. A multivariate data analysis approach. Int. J. Pharm. 237, 193–207.

Pedersen, G.P., Faldt, P., Bergenstahl, B., Kristensen, H.G., 1998. Solid state characterisation of a dry emulsion: a potential drug delivery system. Int. J. Pharm. 171, 257–270.

Saers, E.S., Nystrom, C., Alden, M., 1993. Physicochemical aspects of drug release. 16. The effect of storage on drug dissolution from solid dispersions and the influence of cooling rate and incorporation of surfactant. Int. J. Pharm. 90, 105–118.

Serajuddin, A.T.M., 1999. Solid dispersion of poorly water-soluble drugs: early promises, subsequent problems, and recent breakthroughs. J. Pharm. Sci. 88, 1058–1066.

Smikalla, M.M., Urbanetz, N.A., 2007. The influence of povidone K17 on the storage stability of solid dispersions of nimodipine and polyethylene glycol. Eur. J. Pharm. Biopharm. 66, 106–112.

Spegt, P., 1970. Influence of molecular weight on lamellar structure of polyoxyethylene. Makromol. Chem. 140, 167–173.

Stegemann, S., Leveiller, F., Franchi, D., De Jong, H., Linden, H., 2007. When poor solubility becomes an issue: from early stage to proof of concept. Eur. J. Pharm. Sci. 31, 249–261.

Takeuchi, H., Sasaki, H., Niwa, T., Hino, T., Kawashima, Y., Uesugi, K., Ozawa, H., 1992. Design of redispersible dry emulsion as an advanced dosage form of oily drug (vitamin-E nicotinate) by spray-drying technique. Drug Dev. Ind. Pharm. 18, 919–937.

Urbanetz, N.A., 2006. Stabilization of solid dispersions of nimodipine and polyethylene glycol 2000. Eur. J. Pharm. Sci. 28, 67–76.

Verheyen, S., Blaton, N., Kinget, R., Van Den Mooter, G., 2004. Pharmaceutical performance of solid dispersions containing poly(ethylene glycol) 6000 and diazepam or temazepam. J. Therm. Anal. Calorim. 76, 405–416.